Chapter 12

Microeconomics of cell metabolism

Jumpei F. Yamagishi and Tetsuhiro S. Hatakeyama

Chapter overview

- Section 12.1 provides a concise overview of microeconomics and cell metabolism, introducing the microeconomic concepts as applied to cell metabolism.
- Section 12.2 exemplifies the usefulness of the microeconomics of metabolism, by providing motivating examples from biology and economics: overflow metabolism and Giffen behavior.
- Section 12.3 derives a universal relationship between nutrient response and drug response: a linear response theory of cell metabolism.
- Section 12.4 formulates the global constraint principle for the law of diminishing returns in organismal growth, integrating and generalizing Monod's growth law and Liebig's law of the minimum from the perspective of resource allocation.
- Section 12.5 summarizes the various concepts discussed in this chapter and outlines future perspectives.

12.1 Cell metabolism as an economic consumer

Cells constantly face the challenge of allocating resources. They must distribute limited nutrients and biosynthetic capacity among various metabolic pathways in order to support growth, maintenance, and other functions.

Paul Samuelson famously stated that 'Economics is the study of how societies use scarce resources to produce valuable commodities and distribute them among different people' [1]. In particular, the microeconomic theory of consumer choice offers a mathematical framework for optimized consumption, i.e., the allocation of budget to various goods (see Box 12.A for a brief introduction). However, human economic behavior is often not optimal due to emotional factors, cognitive limitations, and incomplete information, collectively described as *bounded rationality* [2]. In contrast, evolution can drive organisms toward optimality: ideally, intense natural selection would eliminate organisms that exhibit "irrational" behavior under environmental conditions repeatedly encountered throughout evolutionary history, and cells lack emotions. Indeed, the optimality of intracellular metabolic regulation can often be a useful approximation under well-defined conditions [3]. We therefore expect their metabolic strategies to conform more closely to the predictions of optimization theory, and microeconomic theories should be more successful when applied to metabolic systems.

Although a loose analogy between biology and economics has long been proposed that refers to coenzymes as "currency metabolites," we can in fact map metabolism precisely onto the theory of consumer choice (Table 12.1 and Box 12.A) [4, 5, 6]. In this theory which we call the "microeconomics of metabolism," cellular objectives such as growth rate correspond to utility, the intake of a supplied nutrient source is considered as income, and metabolic pathways

Table 12.1: Mapping between microeconomics and cell metabolism

Microeconomics	Cell Metabolism
Utility	Growth Rate
Income	Nutrient Intake
Goods	Metabolic Pathways
Demands	Fluxes of Pathways
Price	Inverse Metabolic Yield
Complementarity	Law of Mass Conservation

and their fluxes correspond to goods and demands, respectively. Regarding price, note that in economics, price quantifies the inverse of the conversion efficiency from income to goods; a higher price reduces the quantity of goods that can be purchased. Similarly, the price of a metabolic pathway corresponds to the inverse of the conversion efficiency of a supplied nutrient into the pathway's products[1].

In microeconomics, the theory of consumer choice especially addresses how consumption behaviors respond to changes in income and price, within the framework of optimization problems (Box 12.A): a key feature of this theory is the separation of the objective function and the budget constraint, which allows for a systematic investigation of perturbation responses. Accordingly, the microeconomics of metabolism allows us to discuss the response of (optimized) metabolic activities to changes in the environment. The following sections demonstrate how an analogous response theory can be constructed for cell metabolism.

12.2 An example: overflow metabolism and Giffen behavior

In this section, we will introduce the microeconomics of metabolism by using overflow metabolism as a motivating example. Overflow metabolism, a recurring topic throughout this book, is a phenomenon in which cells ubiquitously prefer fermentation to more energy-efficient respiration, even in the presence of abundant oxygen. This seemingly wasteful behavior is ubiquitous across species and is also known as the Warburg effect in cancer cells and the Crabtree effect in yeast. It is a useful example for introducing the concepts of economics and trade-offs [4].

We introduce a minimal model consisting of two metabolic pathways. Examining this model first demonstrates that a trade-off between pathways causes overflow metabolism (Figure 12.1). We then show that this framework also yields universal insights into drug responses, such as the drug-induced reverse Warburg effect, from a microeconomic perspective.

12.2.1 Minimal model for overflow metabolism

As a minimal model for overflow metabolism, we consider only two metabolic pathways, respiration and fermentation. Their fluxes, denoted by f_{r} and f_{f}, are constrained by the maximal intake flux I_C of a single nutrient (e.g., glucose or another carbon source) as

$$p_{\mathrm{r}} f_{\mathrm{r}} + p_{\mathrm{f}} f_{\mathrm{f}} \leq I_C, \tag{12.1}$$

which represents the allocation of carbon source intake to respiration pathway (i.e., glycolysis with TCA cycle and oxidative phosphorylation (OXPHOS)) and fermentation pathway (i.e., glycolysis with acetate/lactate secretion). From the perspective of microeconomics, Eq. (12.1) represents the budget constraint for two goods, while the input stoichiometric coefficients p_{r} and p_{f} are interpreted as the "price" of respiration and fermentation pathways, respectively; in other words, the price of a metabolic pathway measures the amount of nutrients required per unit end-product(s) of the pathway, inversely proportional to the yield of those products (see also Section 12.2.3). We normalize these coefficients as $p_{\mathrm{r}} = p_{\mathrm{f}} = 1$ unless otherwise stated.

Cellular growth rate Λ is the objective function. In this minimal model, we coarse-grain cellular growth as being limited by a single biomass synthesis reaction from energy molecules such as ATP (A) and another biomass precursor such as amino acids, nucleic acids, and lipids (B): $A + B \to \mathrm{biomass}\,(\mathrm{BM})$. Since the reactants of a reaction cannot be compensated for each other due to the law of mass conservation [10, 11], cellular growth rate Λ is then determined

[1] The price of metabolic pathways here differs from the enzyme cost discussed in Chapter 6.

Economics box 12.A Microeconomic theory of consumer choice

The standard microeconomic theory of consumer choice provides the mathematical backbone of our framework. This box gives an overview of the key concepts necessary for translating between economic language and metabolism. The theory of consumer choice explains how the price p_i of goods and income I determine consumption behavior, i.e., demand x_i for each good i. The decision-making process for a rational consumer is formulated as an optimization problem of the utility $u(x_1, x_2, \cdots, x_n)$ under the budget constraint $\sum_{i=1}^{n} p_i x_i \leq I$.

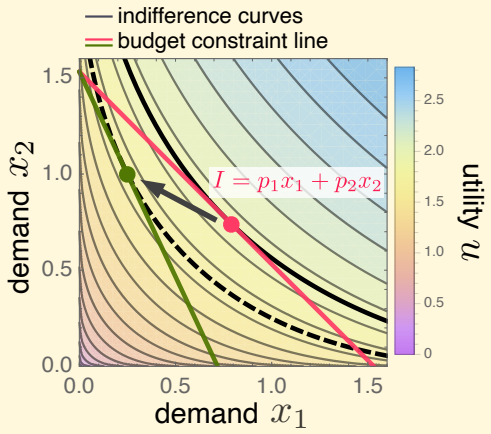

When the number of goods n is two, the utility landscape can be represented as a curved surface, and the demand for each good is basically determined from a tangent point of the budget constraint line, $p_1x_1 + p_2x_2 = I$, to the indifference curve (contour of utility) on which utility u takes the largest value.

The graphics on the left shows an example of a utility landscape, $u(x_1, x_2)$. The contours, called indifference curves in microeconomics, are shown together with the budget constraint line $I = p_1x_1 + p_2x_2$. Optimal consumption behavior occurs at the point where the budget constraint line and the highest attainable indifference curve intersect. Modified from Ref. [4].

Four types of goods in economics. The theory of consumer choice can be viewed as a kind of perturbation response theory, which focuses on how optimal consumption behavior $\hat{\mathbf{x}}(I, \mathbf{p})$ responds to changes in income I and prices $\mathbf{p}$. Typically, an increase in price leads to a decrease in demand. Among such goods, goods for which income increases lead to higher demand are called normal goods, while goods for which income increases lead to lower demand are called inferior goods (see Table below). For instance, both goods 1 and 2 in the Figure above are normal goods. Economic examples of normal and inferior goods are coffee and instant coffee, respectively; in general, cheaper substitutes for non-essential items tend to be inferior goods.

	Income I ↗	Price p_i ↗	Example in economics
Normal goods	Demand x_i ↗	Demand x_i ↘	Coffee
Inferior goods	Demand x_i ↘	Demand x_i ↘	Instant Coffee
Giffen goods	Demand x_i ↘	Demand x_i ↗	?
Veblen goods	Demand x_i ↗	Demand x_i ↗	Branded Item

Giffen goods. Economists also consider a rare class of goods for which demand increases as the price rises. When such goods are also inferior goods, that is, when demand decreases as income rises, they are called Giffen goods. In reality, there are no robust examples at the market level, and only a few cases, such as rice, have been reported at the individual level [7]. By contrast, goods whose demand increases with income are called Veblen goods: branded luxury items, for instance, may exhibit higher demand at higher prices because the higher price itself raises their perceived prestige (see also the explanation of the Slutsky equation on the next page).

as

$$\Lambda(f_\mathrm{r}, f_\mathrm{f}) := \min\left(J_A(f_\mathrm{r}, f_\mathrm{f}), J_B(f_\mathrm{r}, f_\mathrm{f})\right), \tag{12.2}$$

where J_A and J_B denote the production rates of the energy molecule A and the other growth-limiting biomass precursor B, respectively. Note here that different biomass precursors are non-substitutable or complementary; that is, even if one precursor is produced in excess, it does not contribute to biomass synthesis, and the precursor with the lower production rate becomes the rate-limiting factor. This property stems from the law of mass conservation and can be depicted geometrically as a growth-rate landscape with kinked contours, and these kinks form the ridgeline of the growth-rate landscape (Figure 12.1B). From an economic perspective, objective functions that involve a minimum function are known as the Leontief utility functions [7, 4] (see also Box 12.A).

The production rates of ATP (J_A) and other growth-limiting biomass precursors such as amino acids (J_B) are assumed to linearly depend on the fluxes of respiration and fermentation pathways, f_r and f_f, for simplicity. The former is given

Economics box 12.A Microeconomic theory of consumer choice (continued)

Complementarity and Leontief utility function. In economics, it is well known that some goods cannot be substituted for one another. Examples include the left and right shoes of a pair, as well as a camera and film. These goods are complementary, meaning they only perform their intended function when both are present. This property is called complementarity. The utility of such complementary goods can be represented using a minimum function, for example $u(x_1, x_2) = \min(x_1, x_2)$ (see Figure A below). These types of utility functions are called Leontief utility functions and are widely used in input-output analysis in manufacturing and other industries [8, 7]. Leontief utility functions capture the characteristic feature of complementarity exhibited by metabolic systems due to the laws of mass conservation and stoichiometry (see also Chapter 9).

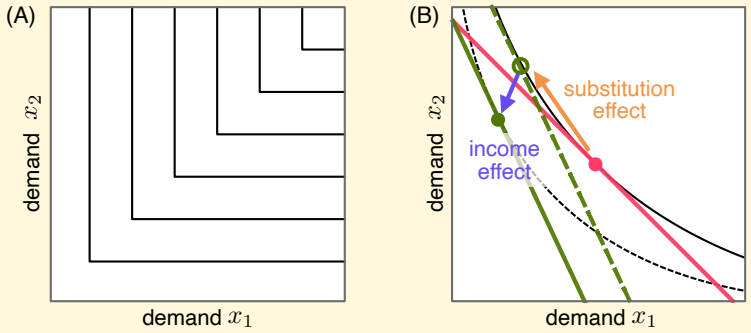

(A) Indifference curves in the Leontief utility function with complementary goods, $u(x_1, x_2) := \min(x_1, x_2)$. (B) Geometric description of substitution effect (orange) and income effect (purple).

Slutsky equation. The influence of a change in price on the demand for goods can be decomposed into two distinct effects, known as the Slutsky equation:

$$\frac{\partial \hat{x}_i(\mathbf{p}, I)}{\partial p_j} = \underbrace{\frac{\partial h_i(\mathbf{p}, \hat{u}(\mathbf{p}, I))}{\partial p_j}}_{\text{[Substitution effect]}} \underbrace{- \hat{x}_j(\mathbf{p}, I) \frac{\partial \hat{x}_i(\mathbf{p}, I)}{\partial I}}_{\text{[Income effect]}},$$

where $h_i(\mathbf{p}, u)$ is defined as the minimum demand for good i to achieve a utility value u and $\hat{u}(\mathbf{p}, I)$ is defined as the maximum utility under a given price $\mathbf{p}$ and income I (see Appendix 12.5.1 for a detailed derivation). The substitution effect is caused by relative changes in the combination of the demand for goods. In contrast, an increase in a good's price effectively decreases the budget to spend freely, thereby altering the demand for each good; this is called the income effect.

Geometrically, the substitution effect is represented by the movement of the demand for goods along the original indifference curve to a point at which the slope of the tangent line equals the ratio of the altered price of the goods. In contrast, the income effect is represented by a downward, parallel shift of the budget constraint line (see Figure B above). If the utility is given as a Leontief utility function, the substitution effect is zero within a certain range of the price change due to the indifferentiability of each indifference curve at the kink [9]. The self-substitution effect is always non-positive in the above formulation [8]. Accordingly, Veblen goods require the price $\mathbf{p}$ to appear in the argument of the utility function as $u(\mathbf{x}, \mathbf{p})$ with $\partial u / \partial p_i > 0$ so that the increase in utility from a price increase is explicitly incorporated.

as

$$J_A(f_\mathrm{r}, f_\mathrm{f}) = a_\mathrm{r} f_\mathrm{r} + a_\mathrm{f} f_\mathrm{f}, \tag{12.3}$$

where a_i denotes ATP yield in pathway i and satisfies $a_\mathrm{r} > a_\mathrm{f} > 0$ because respiration produces a greater amount of ATP than fermentation from the same amount of the carbon source.

Although respiration and fermentation produce energy molecules, they also consume another limited intracellular resource, such as proteome capacity [12, 13], intracellular space [14, 15], membrane surface [16], or the upper bound on heat dissipation [17]. Let $J_{B,\mathrm{tot}} > 0$ denote the maximum achievable rate of biomass-precursor production when

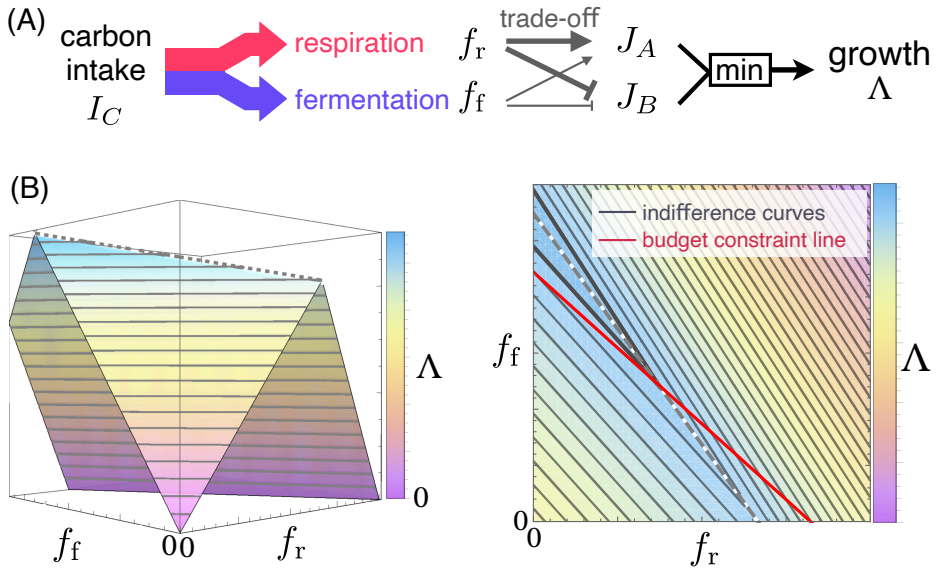

Figure 12.1: Coarse-grained model of overflow metabolism – (A) Schematics of the metabolic model. The supplied carbon source (I_C) is distributed between the respiration and fermentation pathways (f_r and f_f). These two pathways produce energy molecules (J_A) and biomass precursors (J_B), which together determine the cellular growth rate as $\Lambda = \min(J_A, J_B)$. (B) Growth rate landscape (left) and its contour map (right). The grey dashed line is the ridgeline of the growth rate Λ. (Modified from Ref. [4])

all of the limiting resource is allocated to biomass-precursor synthesis. Then, because part of the resource must be allocated to respiration and fermentation pathways, the feasible flux J_B of biomass-precursor production decreases as

$$J_B(f_\mathrm{r}, f_\mathrm{f}) = J_{B,\mathrm{tot}} - b_\mathrm{r} a_\mathrm{r} f_\mathrm{r} - b_\mathrm{f} a_\mathrm{f} f_\mathrm{f}. \tag{12.4}$$

Here, $a_i f_i$ represents the production flux of energy molecules through pathway i, and b_i quantifies the amount of the limiting resource such as proteome capacity, membrane occupancy, or intracellular space consumed per unit energy-molecule flux. Empirical observations suggest that the respiration pathway requires more resources than the fermentation pathway [12, 14, 15, 16, 17], i.e., $b_\mathrm{r} > b_\mathrm{f}$ holds[2]. Consequently, a trade-off between f_r and f_f or J_A and J_B is assumed here (Figure 12.1A).

Finally, we assume that the pathway fluxes, f_r and f_f, are rationally regulated to maximize the cellular growth rate Λ under the above "budget constraint" (Eq. (12.1)). This model can be regarded as a reformulation of the model in Ref. [12] as an optimization problem.

12.2.2 Nutrient response: trade-off leads to overflow metabolism

In this metabolic model, we calculate how the optimal metabolic flux allocation depends on the carbon influx. It reproduces the characteristic behavior of overflow metabolism (Figure 12.2A): the optimized respiration flux $\hat{f}_\mathrm{r}$ initially increases and then decreases with the carbon influx I_C, while the optimized fermentation flux $\hat{f}_\mathrm{f}$ begins to increase at the switching point.

Motivated by biological plausibility, we assumed a trade-off of the form $a_\mathrm{r} > a_\mathrm{f}$ and $b_\mathrm{r} > b_\mathrm{f}$ in Eqs. (12.3-12.4), and showed that this condition reproduces overflow metabolism, namely the switch from respiration to fermentation. Furthermore, this trade-off is not only sufficient but also necessary for overflow metabolism (Problem 12.1).

[2] In this model, the respiration pathway denotes glycolysis combined with the TCA cycle and OXPHOS, whereas the fermentation pathway denotes glycolysis with acetate/lactate secretion. The definitions of these pathways imply that the former consumes more resources than the latter, i.e., $b_\mathrm{r} > b_\mathrm{f}$ (see also Online Resource 1 in Ref. [4] for the estimated parameter values). By contrast, if one compares only the TCA cycle and OXPHOS with (aerobic) glycolysis alone, there is a report that the former is more protein-efficient [18].

In summary, the essential condition for overflow metabolism in this model is a trade-off between the respiration and fermentation pathways[3], regardless of the specific molecular-biological nature of B (and A) [4], as also discussed in Ref. [19]. Such a simple mathematical structure likely underlies the remarkable ubiquity of overflow metabolism across species, from cancer cells to yeasts and prokaryotes, whereas the identity of the growth-limiting biomass precursor B (and the exact values of $b_{\rm r}$ and $b_{\rm f}$) may vary across species and environmental conditions.

12.2.3 Drug response as a Giffen behavior

The responses of metabolic strategies to changes in $p_{\rm r}$ (and $p_{\rm f}$) can also be calculated analytically. In metabolism, a change in price p_i is interpreted as the metabolic inhibition of pathway i, which can be achieved through drug administration.

In economics, the price quantifies the inverse of the efficiency of converting currency into goods: if the price of a good increases, then the consumer can obtain a smaller amount of the good with the same budget. Similarly, the price of a metabolic pathway can be defined as the inverse of the efficiency of converting a nutrient molecule into end-product(s) (see also Table 12.1). That is, the price of respiration pathway, $p_{\rm r}$, is defined as the (effective) input stoichiometric coefficient, i.e., how many units of carbon source are required to produce one unit of ATP. The aforementioned normalization, $p_{\rm r} = p_{\rm f} = 1$, corresponds to a baseline situation without losses due to external manipulation.

With the trade-off, $a_{\rm r} > a_{\rm f}$ and $b_{\rm r} > b_{\rm f}$ in Eqs. (12.3-12.4), the optimized metabolic allocation, denoted by $(\hat{f}_{\rm r}, \hat{f}_{\rm f})$, exhibits the following responses to increases in the price of respiration pathway, $p_{\rm r}$ (Figure 12.2B):

1. Inhibition of respiration (i.e., rise in $p_{\rm r}$) counterintuitively promotes the optimized respiration flux $\hat{f}_{\rm r}$.
   From the perspective of microeconomics, the demand for respiration decreases when income I_C increases (overflow metabolism), while it increases when the price $p_{\rm r}$ rises. Thus, the respiration pathway is classified as a Giffen good (see also Section 12.3.3). Although this Giffen behavior seems counterintuitive, it is universally predicted for metabolic pathways that exhibit a negative nutrient response (i.e., a decrease in pathway flux with increasing nutrient influx), as we discuss in the next subsection.
2. The optimal allocation $(\hat{f}_{\rm r}, \hat{f}_{\rm f})$ discontinuously changes at $p_{\rm r} = a_r/a_f$.
   Intuitively, once the efficiency of the respiration pathway is reduced beyond the threshold by manipulations such as drug treatment, the fermentation pathway becomes more efficient even in terms of ATP production; as a result, respiration is no longer used and cellular metabolism switches completely to fermentation.

From an experimental viewpoint, so-called uncouplers of respiration dissipate the proton gradient to produce ATP, thereby decreasing the metabolic efficiency of energy production [20]; therefore, the administration of such drugs increases the price of respiration. Indeed, both of the above theoretical predictions are qualitatively consistent with experimental data (see, e.g., Figure 2 of Ref. [20]).

12.2.4 Relationship between nutrient response and drug response

The above model captures the essence of overflow metabolism and reveals its conditions, also predicting the counterintuitive promotion of the inhibited respiration pathway. These nutrient responses and inhibitor responses, which are qualitatively different types of metabolic responses, are generally interrelated via the Slutsky equation, a theorem in mathematical economics.

By applying the Slutsky equation (Appendix 12.5.1, Eq. (12.19)) to the above model, we immediately obtain

$$\frac{\partial \hat{f}_i(\mathbf{p}, I_C)}{\partial p_j} = \frac{\partial h_i(\mathbf{p}, \hat{\Lambda}(\mathbf{p}, I_C))}{\partial p_j} - \hat{f}_j(\mathbf{p}, I_C) \frac{\partial \hat{f}_i(\mathbf{p}, I_C)}{\partial I_C}$$

where $(i, j = r, f)$. While the first term (the substitution effect) depends on the details of the utility or growth rate function, it disappears with the Leontief utility function [9].

[3] This is analogous to the concept of comparative advantage in Ricardo's economic theory of international trade.

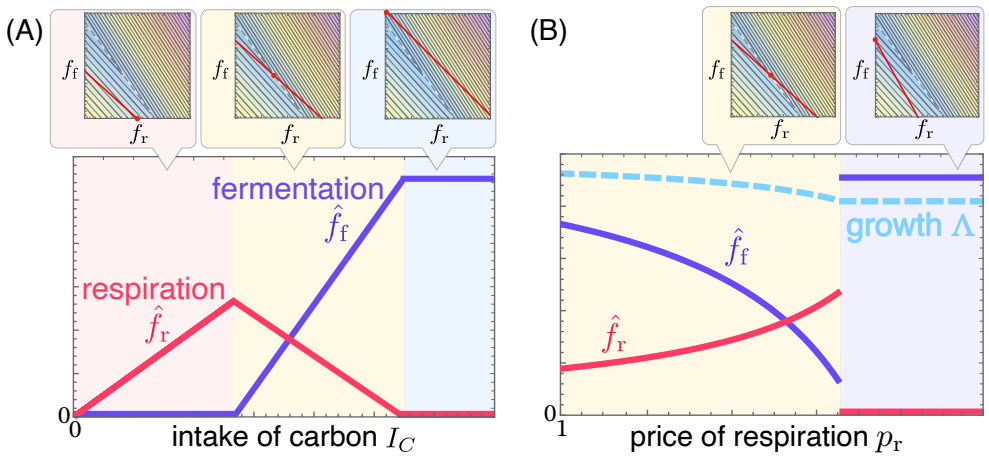

Figure 12.2: Responses of optimal allocation of carbon intake – (A) Dependence of the optimized pathway fluxes, $(\hat{f}_r, \hat{f}_f)$, on the carbon source intake I_C (called Engel curves in microeconomics). Overflow metabolism is reproduced as a result of optimization. (B) Dependence of the optimized pathway fluxes, $(\hat{f}_r, \hat{f}_f)$, and growth rate $\Lambda(\hat{f}_r, \hat{f}_f)$ on the price of respiration pathway, p_r. I_C and $p_f = 1$ are fixed here. (Modified from Ref. [4])

Therefore, we obtain

$$\frac{\partial \hat{f}_i(\mathbf{p}, I_C)}{\partial p_j} = -\hat{f}_j(\mathbf{p}, I_C)\frac{\partial \hat{f}_i(\mathbf{p}, I_C)}{\partial I_C}. \tag{12.5}$$

This equation connects metabolic responses to qualitatively different types of environmental variations or manipulations. The case with $i = j$ is particularly insightful: it then implies that the changes in the optimal flux of pathway i with increasing the price of pathway i, $\partial \hat{f}_i/\partial p_i$, and with increasing the nutrient availability, $\partial \hat{f}_i/\partial I_C$, have opposite signs. Accordingly, respiration is predicted to be activated by uncoupler administration if and only if overflow metabolism occurs under the given environmental conditions.

In the next section, we prove the generalization of Eq. (12.5) to arbitrary metabolic systems and discuss its biological implications in more detail.

12.3 A linear response relation in cell metabolism

This section presents the mathematical derivation of a general linear response relation for metabolism, Eq. (12.15), which universally holds in arbitrary metabolic systems (see also Figure 12.4).

To this end, Section 12.3.1 first introduces a general framework of constraint-based modeling (CBM). We adopt a formulation that incorporates arbitrary constraints, such as proteome constraints and intracellular space constraints, and that uses pathway fluxes instead of reaction fluxes as variables. This formulation remains equivalent to the conventional CBM. Then, we can take advantage of microeconomic concepts to analyze cell metabolism. Within this framework, Section 12.3.2 proves that the Slutsky equation for metabolism (12.5), obtained in Section 12.2.4, is generalized to arbitrary metabolic systems [5]. It serves as a universal linear relation of how the flux of arbitrary metabolic pathway or reaction responds to nutrient availability and drug administration or metabolic inhibition, that is, qualitatively different types of environmental conditions. Finally, Section 12.3.3 explores the biological implications of this universal relation.

12.3.1 Constraint-based modeling in metabolism

To provide a microeconomic formulation of arbitrary metabolic systems, we first introduce the constraint-based modeling (CBM) in systems biology. In the framework of CBM, intracellular resource allocation is formulated as an optimization problem: linear programming (LP) problems in which the variables are the fluxes $\mathbf{v}$ of reactions (see also

Chapter 5, "Optimization of metabolic fluxes") . As discussed below, LP problems in CBM are generally equivalent to optimization problems in the microeconomic theory of consumer choice (see Figure 12.3 and Table 12.2).

In the framework of flux balance analysis (FBA), the most popular method in CBM, the optimized resource allocation is formulated as [21, 22]:

$$\underset{\mathbf{v}}{\text{maximize}}\ \mathbf{c}^\top \mathbf{v}\ \text{ s.t. }\ \sum_{j\in\mathcal{R}} S_{\mu j} v_j = 0\ \ (\mu \in \mathcal{M}) \tag{12.6}$$

$$v_i^{\text{lb}} \le v_i \le v_i^{\text{ub}}, \tag{12.7}$$

where the set of all compounds (metabolites) and metabolic reactions are denoted by $\mathcal{M}$ and $\mathcal{R}$, respectively. Here, $\mathbf{c}$ is a $|\mathcal{R}|$-dimensional vector that specifies the weights of each reaction flux in the objective function. Because $\sum_{j\in\mathcal{R}} S_{\mu j} v_j$ is equal to the excess production of compound μ, Eq. (12.6) represents that the production and degradation of internal metabolites must be balanced at the steady states.

CBM addresses a much broader range of problems than standard FBA, including constraints beyond compound mass balance. The general formulation of CBM can be represented as (see also Figure 12.3A):

$$\underset{\mathbf{v}\ge\mathbf{0}}{\text{maximize}}\ \mathbf{c}^\top \mathbf{v}\ \text{ s.t. }\ \sum_{j\in\mathcal{R}} S_{\mu j} v_j = 0\ \ (\mu \in \mathcal{M}\backslash\mathcal{E}) \tag{12.8}$$

$$\sum_{j\in\mathcal{R}} S_{\alpha j} v_j + I_\alpha \ge 0\ \ (\alpha \in \mathcal{E}\cup\mathcal{C}), \tag{12.9}$$

where a non-negative vector $\mathbf{v} := \{v_i\}_{i\in\mathcal{R}}$ represents the fluxes of all reactions, by decomposing each reversible reaction into two irreversible reactions (i.e., its forward and backward components). This approach is useful for further clarifying the correspondence between economic demands and metabolic fluxes.

With respect to Eq. (12.9), if α is a compound ($\alpha \in \mathcal{E} \subset \mathcal{M}$), the corresponding inequality, $\sum_{j\in\mathcal{R}} S_{\alpha j} v_j + I_\alpha \ge 0$, represents that exchangeable compound α with intake $I_\alpha > 0$ can be imported and compound α with efflux $I_\alpha < 0$ are (forcibly) leaked or degraded; in contrast, if α is a constraint ($\alpha \in \mathcal{C}$), it represents a non-stoichiometric constraint, e.g., allocation of some limited resource such as proteins [12, 13], intracellular space [14, 15], membrane surface [16], and Gibbs energy dissipation [17]. Note that $\mathcal{C}$ can also include other constraints like the upper and lower bounds of the flux of reaction i: the inequalities in Eq. (12.7) can be represented as two constraints, $\sum_j S_{(i,\text{lb}),j} v_j + I_{(i,\text{lb})} \ge 0$ with $I_{(i,\text{lb})} := -v_i^{\text{lb}}, S_{(i,\text{lb}),i} := 1, S_{(i,\text{lb}),j} := 0\,(j \ne i)$ and $\sum_j S_{(i,\text{ub}),j} v_j + I_{(i,\text{ub})} \ge 0$ with $I_{(i,\text{ub})} := v_i^{\text{ub}}, S_{(i,\text{ub}),i} := -1, S_{(i,\text{ub}),j} := 0\,(j \ne i)$.

CBM with pathway fluxes $\mathbf{f}$ as variables The LP problem (12.8-12.9) with reaction fluxes $\mathbf{v}$ as variables can be equivalently transformed into a LP problem with pathway fluxes $\mathbf{f}$ as variables (see also Figure 12.3). The latter formulation provides a clearer picture when mapping the theory of consumer behavior onto cell metabolism.

A metabolic pathway means a linked sequence of reactions and is defined by a *pathway matrix* $P := \{P_{ii'} \ge 0 \mid i \in \mathcal{R}, i' \in \mathcal{P}\}$ which represents that pathway i' comprises $P_{ii'}$ units of reaction i, and pathway fluxes $\mathbf{f}$ are related to reaction fluxes as $\mathbf{v} = P\mathbf{f}$.

P should be chosen as (linear combinations of) elementary flux modes (EFMs) or extreme rays of the flux cone, so that the balance of internal compounds (12.8) is autonomously satisfied (see also Chapter 4, "Metabolic flux distributions"). That is, P should be chosen as

$$\sum_{j\in\mathcal{R}} S_{\mu j} \left(P\mathbf{f}\right)_j = 0\ \ (\mu \in \mathcal{M}\backslash\mathcal{E}) \tag{12.10}$$

holds with arbitrary $\mathbf{f} := \{f_{i'} \ge 0\}_{i'\in\mathcal{P}}$.

Let us then consider two stoichiometry matrices for reactions $\mathcal{R}$ and pathways $\mathcal{P}$, S and K, respectively (see also Table 12.2). For compound $\alpha\,(\in \mathcal{M})$, $|S_{\alpha i}|$ represents the number of units of compound α produced if $S_{\alpha i} > 0$ and consumed if $S_{\alpha i} < 0$ in reaction i; whereas if α denotes a constraint ($\alpha \in \mathcal{C}$), $S_{\alpha i}$ is usually negative and $|S_{\alpha i}|$ repre-

sents the number of units of constraint α required for reaction i. The stoichiometry matrix K for metabolic pathways $\mathcal{P}$ is also defined similarly. Throughout this Chapter, we use indices with primes such as i' to denote pathways and those without primes such as i to denote reactions, and $|S_{\alpha i}|$ and $|K_{\alpha i'}|$ are called input (output) stoichiometric coefficients of reaction i and pathway i', respectively, if $S_{\alpha i}$ and $K_{\alpha i'}$ are negative (positive). Notably, the stoichiometry matrix K for pathways, defined as $K := SP$, represents metabolic pathways in "compound space" and corresponds to the elementary conversion modes [23].

With these definitions, the LP problem (12.8-12.9) for CBM can be rewritten into another LP problem with pathway fluxes $\mathbf{f}$ as variables:

$$\begin{aligned} &\underset{\mathbf{f}\geq\mathbf{0}}{\text{maximize}}\ \mathbf{c'}^{\top}\mathbf{f} \\ &\text{s.t.}\quad \sum_{j'\in\mathcal{P}} K_{\alpha j'} f_{j'} + I_\alpha \geq 0 \ \ (\alpha \in \mathcal{E}\cup\mathcal{C}) \end{aligned} \tag{12.11}$$

where $\mathbf{c}'$ is defined as $\mathbf{c'}^{\top} := \mathbf{c}^{\top} P$, and $\mathcal{E}\ (\subset \mathcal{M})$ denotes the set of exchangeable compounds that are transported through the cellular membrane. This LP problem represents the optimization of how to allocate each resource α while satisfying constraint (12.11), which reflects that the total consumption of a compound cannot exceed its intake.

As a simple example, the coarse-grained microeconomic model in Section 12.2 (Figure 12.1) is equivalent to the CBM problem with the stoichiometry matrix, $K \in \mathbb{R}^{(\mathcal{M}\cup\mathcal{C})\times\mathcal{P}}$, where $\mathcal{M} = \{C, A\}$, $\mathcal{C} = \{B\}$, and $\mathcal{P} = \{\mathrm{r}, \mathrm{f}, o\}$:

$$K = \begin{pmatrix} -p_\mathrm{r} & -p_\mathrm{f} & 0 \\ a_\mathrm{r} & a_\mathrm{f} & -1 \\ b_\mathrm{r} & b_\mathrm{f} & -1 \end{pmatrix}.$$

Microeconomic formulation of metabolic resource allocation When cells are assumed to maximize the flux of a single objective reaction $o\ (\in\mathcal{R})$ such as biomass synthesis in reproducing cells and ethanol or ATP synthesis in metabolically engineered cells (i.e., when c_i is positive only for the objective reaction $i = o$), the correspondence with microeconomics becomes more explicit (see also Figure 12.3). For convenience, we also define the set of the compounds consumed in and the components required for reaction o as objective components $\mathcal{O}\ (\subset \mathcal{M}\cup\mathcal{C})$; thus, $S_{\alpha o}$ for each objective component $\alpha\ (\in\mathcal{O})$ is negative.

In this case, LP problem (12.11) with pathway fluxes $\mathbf{f}$ as the variables is equivalent to the following LP problem:

$$\begin{aligned} &\underset{\Lambda,\mathbf{f}\geq\mathbf{0}}{\text{maximize}}\ \Lambda \\ &\text{s.t.}\quad \sum_{j'\in\mathcal{P}} K_{\alpha j'} f_{j'} + I_\alpha \geq -S_{\alpha o}\Lambda \ \ (\alpha \in \mathcal{E}\cup\mathcal{C}), \end{aligned} \tag{12.12}$$

where $\Lambda := \hat{v}_o$.

Here, the min function for the objective function, $\Lambda := \min(A, B)$, can be replaced by constraints of $\Lambda \leq A$ and $\Lambda \leq B$. Therefore, the optimization problem in CBM (12.11) is equivalent to the maximization of the following Leontief utility function, i.e., the minimum of multiple "complementary" objectives:

$$\Lambda(\mathbf{f}) := \min_{\alpha\in\mathcal{O}} \left[\frac{1}{-S_{\alpha o}} \left(\sum_{j'\in\mathcal{P}} K_{\alpha j'} f_{j'} + I_\alpha \right) \right], \tag{12.13}$$

under the constraints for the available pathway fluxes **f**,

$$-\sum_{j'\in\mathcal{P}} K_{\alpha j'} f_{j'} \leq I_\alpha. \quad (\alpha \in \mathcal{E}\cup\mathcal{C}\backslash\mathcal{O}) \tag{12.14}$$

If compound α (e.g., ADP) is produced by objective reaction o, an additional term $+S_{\alpha o}\Lambda$ appears on the right-hand side of Eq. (12.14), effectively increasing the intake I_α. However, this is not the case for most compounds, including typical nutrients such as glucose.

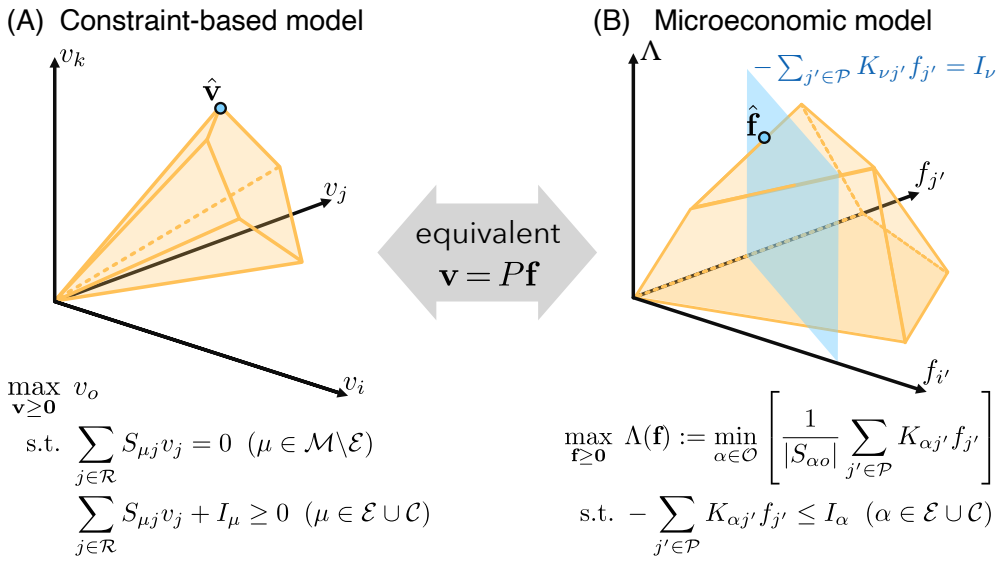

Figure 12.3: Equivalence between a Constraint-Based Model (CBM) and microeconomics – (A) CBM formulation of metabolism with reaction fluxes **v** as variables. The solution subspace (convex set of possible allocations), called the flux cone, is shown in orange. (B) Microeconomic formulation with pathway fluxes **f** as variables and an objective flux Λ. The orange area in **f**-plane (bottom surface) represents the solution subspace, whereas the blue plane vertical to **f**-plane denotes the budget constraint line for a component ν. The blue points $\hat{\mathbf{v}}$ and $\hat{\mathbf{f}}$ represent the optimized fluxes of reactions and pathways, respectively. Given $\mathbf{v} = P\mathbf{f}$ with pathway matrix P, both formulations are equivalent optimization problems. (Modified from Ref. [5])

The min function (12.13) means that the flux of objective reaction o is limited by the minimum available amount of objective components $\mathcal{O}$, reflecting the law of mass conservation, or the complementarity in metabolism. The arguments represent the net production fluxes of "precursors": if α is a metabolite ($\alpha \in \mathcal{M}$), I_α is its intake flux and $\sum_{j'} K_{\alpha j'} f_{j'}$ represents its total production rate; if α is a constraint ($\alpha \in \mathcal{C}$), I_α is the total capacity for constraint α and $\sum_{j'} K_{\alpha j'} f_{j'} + I_\alpha$ is the amount of α that can be allocated to the objective reaction.

This optimization problem (12.13-12.14) can be interpreted as a microeconomic problem in the theory of consumer choice [9, 8], considering $\Lambda(\mathbf{f})$ as the utility function (see also Table 12.1). Inequality (12.14) is interpreted as the budget constraint for each exchangeable compound ν (especially if $K_{\nu j'} \leq 0$ for all pathways j'): e.g., if ν is glucose, the corresponding inequality (12.14) represents carbon allocation. Typically, we focus on a single compound ν as the nutrient, and then, inequalities (12.14) for the remaining exchangeable compounds determine the solution space (Figure 12.3). Here, the maximal intake I_ν of ν corresponds to the income, and the input stoichiometric coefficient for each pathway, $p^\nu_{j'} := -K_{\nu j'}$, serves as the price of pathway j' in terms of ν.

Table 12.2: Symbols in Section 12.3

Symbol	Description
$\mathcal{M}, \mathcal{C}, \mathcal{R}, \mathcal{P}$	Set of compounds / constraints / reactions / pathways
$\mathcal{E}, \mathcal{O}$	Set of exchangeable compound ($\mathcal{E} \subset \mathcal{M}$) / objective components ($\mathcal{O} \subset \mathcal{M}\cup\mathcal{C}$)
S, K	Stoichiometry matrix for reactions / pathways ($S_{\alpha i}, K_{\alpha i'} \in \mathbb{R}; \alpha \in \mathcal{M}\cup\mathcal{C}, i \in \mathcal{R}, i' \in \mathcal{P}$)
$v_i, f_{i'}$	Non-negative flux of reaction $i\,(\in \mathcal{R})$ / pathway $i'\,(\in \mathcal{P})$
$q^\nu_i, p^\nu_{i'}$	Metabolic price of reaction i / pathway i' in terms of $\nu\,(\in \mathcal{M}\cup\mathcal{C})$
I_α	Maximal intake of compound $\alpha\,(\in \mathcal{M})$ or total capacity for constraint $\alpha\,(\in \mathcal{C})$
Λ	Flux of objective reaction $o\,(\in \mathcal{R})$

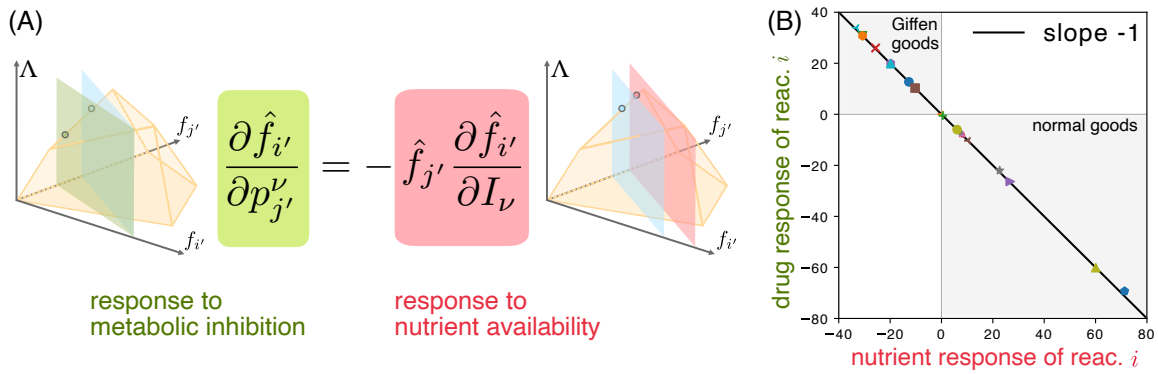

Figure 12.4: Linear response relation for metabolism – (A) Relation between the responses of pathway or reaction flux to metabolic inhibition (green) and to changes in nutrient conditions (red) (Eqs. (12.15) and (12.16)). In the microeconomic interpretation, the response to a drug/inhibitor and nutrient availability corresponds to the response to an increase in prices and income, respectively. (B) Numerical simulations using the *E. coli* core model [24] illustrate that linear response relation of reaction fluxes (12.16) holds. Different colors and marker shapes correspond to different reactions. The black line with slope -1 indicates the exact linear response relation of reaction fluxes (Eq. (12.16)). See also Appendix 12.5.3 and Figure 12.8. (Modified from Ref. [5])

12.3.2 Linear response relation of metabolic pathways

Because Eqs. (12.13-12.14) can be interpreted as a microeconomic optimization problem, we can apply and generalize the Slutsky equation in the theory of consumer choice [8]. In metabolism, it corresponds to the relationship between the responses of the pathway fluxes $\hat{\mathbf{f}}$ (Figure 12.4), as also shown in Section 12.2.4 for a coarse-grained model:

$$\frac{\partial \hat{f}_{i'}}{\partial p^{\nu}_{j'}} = -\hat{f}_{j'}\frac{\partial \hat{f}_{i'}}{\partial I_{\nu}}. \tag{12.15}$$

The right-hand side represents the responses of pathway i' against increases in I_ν, whereas the left-hand side represents those against metabolic inhibitions in pathway j' because the price $p^{\nu}_{j'} = -K_{\nu j'}$ quantifies the inverse of the conversion efficiency from substrate ν to end-products in pathway j'.

In general, the metabolic state of a cell varies depending on intracellular metabolic networks and environmental conditions. Nevertheless, by focusing on the perturbation response of metabolic systems, rather than their states themselves, this linear response relation offers universal predictions independent of the details of metabolic systems. Intuitively, this is because, in metabolism, the law of mass conservation acts as a universal constraint on the responses, and this confines the solutions to an edge of the growth rate landscape (Figure 12.4).

The linear response relation (12.15) serves as a quantitative guide for manipulating the metabolic states of not only model organisms but also non-model organisms toward the desirable directions in microbiology, metabolic engineering, and medicine, as it offers quantitative predictions without prior knowledge of the systems.

Note. Ref. [5] derived Eq. (12.15) by assuming a single objective reaction and directly applying the Slutsky equation. Using the implicit function theorem, we can prove exactly the same relation, without restricting the objective to a single reaction flux (see Appendix 12.5.2 for the derivation). This proof provides a more straightforward derivation and yields a more general response relation: whereas in Ref. [5] the objective function was arbitrary only within the class of single reactions, the present proof remains valid even when the objective function is any linear combination of reaction or pathway fluxes.

Therefore, although the biomass synthesis reaction flux v_o is considered as the objective in Figure 12.4B, the above argument is equally valid when the objective function is the total production flux of some compounds such as ATP or ethanol, as is often considered for metabolically engineered cells [25, 26, 27].

Linear response relation of metabolic reaction fluxes Although Eq. (12.15) generally holds for arbitrary metabolic pathways, it may be experimentally easier to manipulate a single metabolic reaction. Manipulation of a single reaction can affect multiple pathways because they are often tangled via a common reaction in the metabolic network. Hence, another linear response relation closed only for the reaction fluxes $\mathbf{v}$ is useful for application without the need to know the details of the metabolic systems.

By considering effective changes in the stoichiometric coefficients $S_{\alpha i}$ for reaction i as metabolic inhibitions (e.g., inhibition of enzymes, administration of metabolite analogs, leakage of metabolites, and inefficiency in the allocation of some resource), we obtain an equation for the optimized reaction fluxes $\hat{\mathbf{v}}$, formally similar to Eq. (12.15) (see Appendix 12.5.3 for derivation):

$$\frac{\partial \hat{v}_i}{\partial q_i^\nu} = -\hat{v}_i \frac{\partial \hat{v}_i}{\partial I_\nu}. \tag{12.16}$$

We here define the price q_i^ν of reaction i in terms of ν as a function of S, instead of the price $p_{i'}^\nu$ of pathway i' as a function of K,

$$q_i^\nu := \sum_{\alpha \in \mathcal{M} \cup \mathcal{C}} -S_{\alpha i} c_\alpha^\nu(i), \quad c_\alpha^\nu(i) := \frac{\partial \hat{v}_i / \partial I_\alpha}{\partial \hat{v}_i / \partial I_\nu}. \tag{12.17}$$

The coefficient $c_\alpha^\nu(i)$ quantifies the number of units of component ν that can compensate for one unit of α in reaction i. In principle, it is experimentally measurable: for example, if ν is glucose and α is another metabolite such as an amino acid, c_α^ν indicates how many units of glucose are required to compensate for one unit of the amino acid, similar to the "glucose cost" in previous studies [28].

Notably, in the linear response relations (12.15-12.16), calculating only the change in metabolic price is sufficient, rather than the absolute value of the metabolic price itself.

12.3.3 Ubiquity of Giffen goods in cell metabolism

In economic terms, the linear response relation (12.15-12.16) implies that each metabolic pathway must behave either as a normal good or as a Giffen good: as a direct consequence of the law of mass conservation, the income effect and the price response of any metabolic pathway always have opposite signs. While Giffen goods, those whose demand increases when their price rises but decreases when income rises, are extremely rare in human economies (see also Box 12.A), Eqs. (12.15) and (12.16) suggest that Giffen goods are ubiquitous in metabolism: whenever a metabolic pathway decreases its flux in response to increasing nutrient availability, it necessarily behaves as a Giffen good.

Besides respiration pathway in overflow metabolism, the study of cancer metabolism has suggested that several metabolic pathways or reactions tend to be downregulated in fast-growing, nutrient-rich conditions (i.e., exhibit negative nutrient responses). Potential examples include the anaplerotic pathway from glutamine into the TCA cycle (glutamine anaplerosis) [29], pyruvate carboxylation [30], serine catabolism to glycine and formate [31], and the hexosamine biosynthetic pathway [32]. Then, our framework offers a testable prediction: inhibiting these pathways, typically by administration of a metabolic analog or genetic manipulation, can enhance their fluxes.

Furthermore, Section 12.2.2 showed that a trade-off between distinct, yet functionally redundant, metabolic pathways results in a negative nutrient response like the respiration pathway in overflow metabolism. Therefore, when two pathways exhibit such a trade-off, one of them is expected to behave as a Giffen good. Besides respiration and fermentation pathways, a potential example of such pairs is the Embden–Meyerhof–Parnas (EMP) and Entner–Doudoroff (ED) glycolytic pathways [33, 34] (see also Figure 6.1): the EMP pathway is more efficient for ATP production but requires a greater amount of enzymes than the ED pathway; as expected from this trade-off, the ED pathway is utilized to catabolize glucose at high growth rates [33], and thus the EMP pathway is expected to behave as a Giffen good. Other potential examples include a trade-off in ATP production and enzyme occupancy between mixed-acid and lactic-acid fermentation pathways [35] and trade-offs between carbon fixation and light harvesting arising from the allocation of nitrogen between Rubisco and chlorophyll [36].

From an evolutionary standpoint, we expect such trade-offs to be common in evolved metabolic systems. For any pair of redundant pathways or reactions that produce the same metabolite(s), the absence of a trade-off would render one pathway strictly inferior, making its long-term evolutionary maintenance unlikely. Combining this observation with the linear response relation (12.15-12.16), we predict that Giffen goods should be ubiquitous in metabolism. This prediction is not only theoretically non-trivial, but also has concrete experimental implications: many metabolic pathways and reactions are expected to exhibit the counterintuitive promotion of flux upon metabolic inhibition. Lastly, Giffen behavior may be interpreted as a mechanism of homeostasis, whereby the loss of efficiency in a pathway is compensated by an increase in its flux.

12.4 Law of diminishing returns in cell growth

Section 12.3 derived a universal law for the local metabolic responses to small environmental perturbations. In this section, we examine how cellular growth depends on large variations in nutrient availability, and prove that the metabolic allocation of various resources such as nutrients and enzymes generally leads to the law of diminishing returns in cellular growth, as exemplified by Monod's growth law [37].

The question of how cell growth depends on the amount of available nutrients is central to biology. The classical phenomenology, originally proposed by Monod in the 1940s [37], states that microbial growth kinetics, namely the dependence of the specific growth rate μ on substrate availability, generally follows the Monod equation:

$$\mu(s) = \mu_{\text{max}} \frac{s}{K_{\text{S}} + s}, \tag{12.18}$$

where μ_{max} is the maximum growth rate and s is the environmental concentration of the growth-limiting substrate S with its half-saturation concentration K_{S}. Although this phenomenological law is widely accepted empirically, its underlying mechanisms have long remained elusive, which limits the universality and extensibility of the law.

The mechanistic basis for how the substrate limits growth is typically explained by a local biochemical bottleneck. Since the Monod equation has the same functional form as the Michaelis–Menten equation, a single biochemical process is usually assumed to locally limit cell growth [38, 39, 40, 41] (see also Figure 12.5A). In previous hypotheses, this single "black box" could be the substrate transport into cells [42, 38], the net flux of respiration [43], or the reaction that couples catabolism and anabolism [44].

However, microbial growth is achieved collectively by the interplay of thousands of biochemical processes. There is considerable experimental evidence that cell growth is not limited by a single biochemical process alone [45, 46]: for example, experimental changes in the environmental conditions of nitrogen sources can alter the dependence of growth rate on the availability of carbon sources [47, 48]; and cells exhibit qualitatively different phenotypes with respect to the metabolism of nutrients for cell growth [21].

In addition, the accumulation of experimental data has shown that the observed microbial growth kinetics are not accurately captured by the Monod equation [38, 49, 50, 51]. That is, the shape of actual microbial growth kinetics curves varies across species and environments and there is no longer quantitative evidence to support the exact functional form of Eq. (12.18). Nevertheless, certain features still appear to be universal [38, 49, 51]: (i) growth rate is a monotonically increasing function of nutrient availability and (ii) growth rate exhibits concavity with respect to nutrient availability[4], in other words, there are diminishing returns to getting more and more of a nutrient.

A novel macroscopic framework is thus needed to elucidate the underlying mechanism of these fundamental features (i-ii) in microbial growth.

[4] Empirically, there can be a limited minimum substrate concentration s_{min} to achieve cell growth due to the maintenance energy requirements [50, 46]. However, in classical arguments such as Monod's, they are effectively ignored for simplicity by considering the substrate concentration s after subtracting s_{min}.

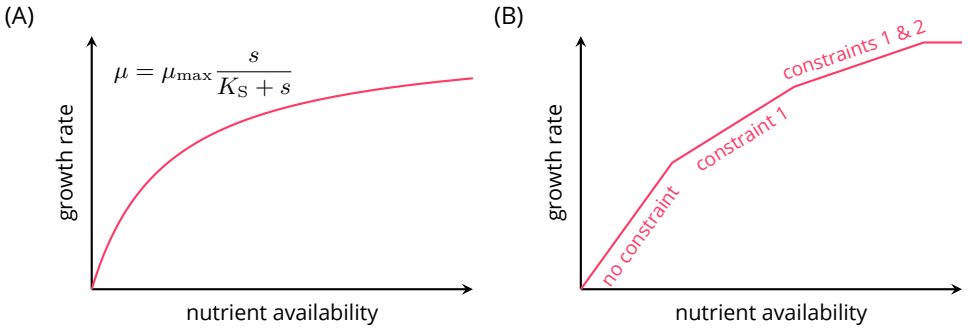

Figure 12.5: Microbial growth kinetics: law of diminishing returns in cell growth – (A) Monod's microbial growth model. (B) Global constraint principle for the microbial growth kinetics curve. (Modified from Ref. [6])

12.4.1 Global constraint principle for microbial growth law

We here propose the global constraint principle for the law of diminishing returns in cellular growth: as the availability of a specific nutrient increases, some other resources are gradually depleted and act as additional growth-limiting factors (see also Figure 12.5B).

From a mathematical standpoint, the dual problem of the LP formulation of CBM (Eqs. (12.8–12.9)) is useful for showing concavity of the optimal growth rate $\mu := \hat{v}_o$, or the law of diminishing returns in cellular growth:

$$\begin{aligned} \underset{\mathbf{y}\in\mathbb{R}^{\mathcal{M}\cup\mathcal{C}}}{\text{minimize}} \sum_{\alpha\in\mathcal{E}\cup\mathcal{C}} I_\alpha y_\alpha \quad \text{s.t.} \qquad & -\sum_\alpha S_{\alpha o} y_\alpha \geq 1, \\ & -\sum_\alpha S_{\alpha i} y_\alpha \geq 0 \;\; (i \neq o), \\ & y_\alpha \geq 0 \;\; (\alpha \in \mathcal{E}\cup\mathcal{C}). \end{aligned}$$

Note that the nutrient availability $\mathbf{I}$ changes the feasible solution space of the primal problem (Eqs. (12.8–12.9)), whereas it does not affect that of the dual problem because $\mathbf{I}$ appears only in the coefficients of the objective function to be minimized in the dual problem. The optimized dual variables, $\hat{y}_\alpha$, are called shadow prices and represent the rate at which the optimal growth rate changes in response to a one-unit increase in the influx of metabolite α. From the strong duality theorem $\hat{v}_o = \sum_\alpha I_\alpha \hat{y}_\alpha$, $\hat{y}_\alpha = \partial\mu/\partial I_\alpha$ holds. We can mathematically prove that $\hat{y}_S$ gradually diminishes with increasing the availability I_S of focal nutrient S (Problem 12.2)[5].

This suggests that Monod's growth law may be better understood as a consequence of global resource allocation, rather than a single growth-limiting process as traditionally believed (Figure 12.5). The above argument suggests that monotonicity and concavity are the only universal features commonly shared across systems, while more detailed quantitative features inevitably depend on the molecular-biological specifics of each system.

Schematics: terraced Liebig's barrel The global constraint principle can be interpreted schematically as a modified form of Liebig's law/barrel (Figure 12.6), which we already discussed in Chapter 9: as a nutrient S is poured into the barrel, the surface height corresponds to the growth rate μ, where the height of each stave represents the availability of each resource other than S. The water surface area in the barrel is therefore $\partial I_S/\partial\mu$, which coincides with the inverse of the shadow price $\hat{y}_S = \partial\mu/\partial I_S$ (i.e., the slope of the growth kinetics curve). Each stave spreads out in a stepwise manner, reflecting the metabolic shifts to pathways with lower growth yield from S due to additional global constraints.

[5] More broadly, the same conclusion holds for convex optimization problems in general (see SI Appendix of Ref. [6]).

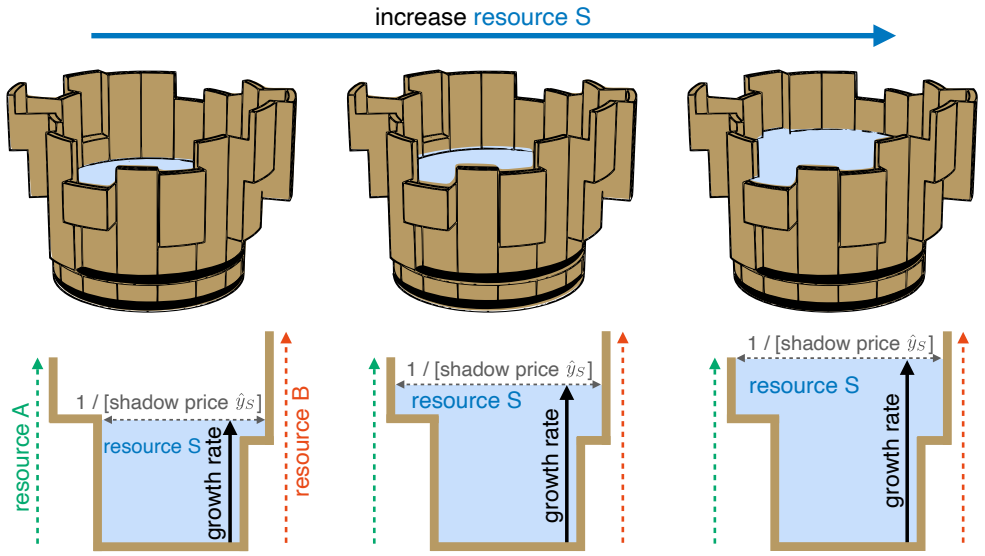

Figure 12.6: Liebig's barrel – The schematics shows a terraced Liebig's barrel (top) and its sectional view for the case with a focal substrate S and the other resources A and B (bottom). (Modified from Ref. [6])

12.4.2 Growth rate dependence on multiple nutrients

The global constraint principle not only captures the law of diminishing returns, but also provides a useful framework for analyzing cell growth under multiple nutrient limitation (Figure 12.7).

Since the growth kinetics curve $\mu(I_S; \tilde{\mathbf{I}})$ is shaped by the global regulation of intracellular metabolism, it depends not only on the availability of the focal nutrient S but also on that of the other resources, here denoted as $\tilde{\mathbf{I}}$. If the availability of a non-focal resource, i.e., a resource other than S, increases (decreases), the constraint on the allocation of the non-focal resource is relaxed (tightened); as a result, the growth kinetics curve $\mu(I_S; \tilde{\mathbf{I}})$ should shift up (down) in the phase(s) where cell growth is limited by the non-focal resource (see also Figure 12.7C). Conversely, by measuring how the shape of the microbial growth kinetics curve responds to environmental manipulations, such as the addition of a nutrient to the medium, one can empirically infer the growth-limiting factors under the original environmental conditions.

Such responses of the microbial growth kinetics curve are indeed observed numerically (Figure 12.7). The decrease in the availability of a non-focal resource, oxygen I_{ox} (Figure 12.7A) or a nitrogen source (ammonium) I_{amm} (Figure 12.7B), shifts the growth kinetics curve $\mu(I_{\mathrm{glc}})$ downward in a phase with sufficiently large I_{glc}, while maintaining the same slope $\hat{y}_S = \partial\mu/\partial I_S$ until the initial downward shift. Then, one can empirically conclude that cell growth in this phase is limited by the non-focal resource under the original environment.

These behaviors, which Monod's law does not capture, are experimentally testable. Indeed, a nitrogen-limited chemostat experiment [52] shows qualitatively consistent trends: reducing the availability of ammonia (the nitrogen source) availability shifts the growth curve $\mu(I_{\mathrm{glc}})$ downward, while leaving the initial (low-I_{glc}) slope essentially unchanged across nitrogen conditions.

12.5 Concluding remarks

In this chapter, we have argued that viewing resource allocation in cell metabolism through a microeconomic lens provides a variety of conceptual and quantitative insights. The interdisciplinary perspective of the microeconomics of metabolism offers several advantages.

Owing to the precise mathematical correspondence summarized in Table 12.1, theorems and definitions from microeconomics can be transferred directly to metabolism. We have used concepts from microeconomics, such as the Slutsky equation, Giffen goods, Leontief utility functions, shadow price, and the law of diminishing returns, to reveal

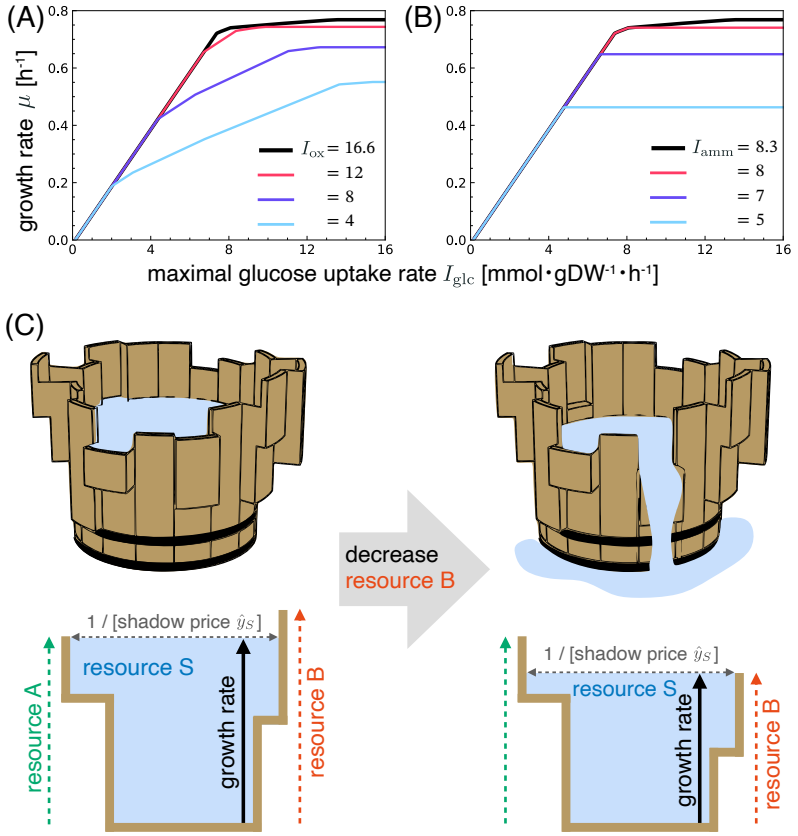

Figure 12.7: Growth rate μ as a function of carbon source availability I_{glc} with different maximal influxes of (A) oxygen I_{ox} and (B) nitrogen source I_{amm}. The dashed lines correspond to the case with $I_{\mathrm{ox}} = 16.6$ and $I_{\mathrm{amm}} = 8.3$. Numerical calculations of Constrained Allocation FBA (CAFBA) [13] were performed using the genome-scale *E. coli* iJO1366 model [53] and the COBRApy package [54]. (C) Schematics with terraced Liebig's barrels (see also Figure 12.6). (left) The shortest stave corresponds to the least available resource A (for example, total proteome in panels A and B), which determines the maximum growth rate. (right) When the availability of resource B (for example, oxygen or ammonia in panels A and B, respectively) decreases, the maximum growth rate is limited by B. This decrease leads to the reallocation of B to metabolic processes and the resulting decrease in the shadow price $\hat{y}_S = \partial\mu/\partial I_S$ at a lower I_S. (Modified from Ref. [6])

a trade-off as the general condition for overflow metabolism (Section 12.2), derive a linear response relation for cell metabolism (Section 12.3), and establish the global constraint principle for cellular growth (Section 12.4). These results illustrate how income and price responses in the microeconomic theory of consumer choice map onto nutrient responses and drug responses in metabolism. Looking ahead, further analysis of metabolic adaptation and regulation using tools from parametric programming and duality theory appears promising.

Notably, in biochemical systems including metabolic systems, physicochemical constraints such as mass conservation and thermodynamic feasibility often enable more general and stronger statements than are available in typical economic settings. While our discussion has focused primarily on cellular metabolism, the underlying principles should, in principle, extend to multicellular systems such as plants and ecosystems; this mirrors the way in which Liebig's law, originally formulated for plant growth, also applies to microbial growth. Thus, the microeconomics of metabolism may ultimately serve as a theoretical basis not only for the metabolism of unicellular organisms, including microbes and cancer cells, but also for that of multicellular organisms and ecological communities.

From a broader and longer-term perspective, the analogy between economics and metabolism appears intellectually fruitful in both directions. As seen in this Chapter, the parallel between budget constraints and cellular resource limitations brings new ways of thinking about metabolic regulation. Recent work has also derived a trade-off between metabolic controllability and thermodynamic cost, by examining the coupling among various currency metabolites

such as ATP, GTP, and NAD(P)H from the perspectives of microeconomics and nonequilibrium chemical thermodynamics [55]. Conversely, insights from metabolic systems, such as the parallel between Giffen goods and the respiration pathway, may, in turn, inspire new questions and analytical frameworks in economic systems, including manufacturing and supply networks.

Recommended readings

"Foundations of Economic Analysis" by P. A. Samuelson (Harvard University Press, 1947) [56]. This book, based on Samuelson's 1941 doctoral dissertation, is a milestone in the field of mathematical microeconomics.

"Energy metabolism of the cell: a theoretical treatise" by J. G. Reich and E. E. Selkov (Academic Press, 1981) [38]. This book brilliantly presents a variety of biological phenomena and theoretical models related to energy metabolism.

Problems

Problem 12.1 Analysis of the coarse-grained model in Section 12.2

(1) Calculate the optimal fluxes $(\hat{f}_{\mathrm{r}}(I_C, p_{\mathrm{r}}, p_{\mathrm{f}}), \hat{f}_{\mathrm{f}}(I_C, p_{\mathrm{r}}, p_{\mathrm{f}}))$ in the coarse-grained model in Section 12.2.

(2) Show the necessary and sufficient condition for overflow metabolism.

Problem 12.2 Proof of convexity in CBM

Prove the convexity of $\mu(\mathbf{I})$ in the LP problem for CBM (Eqs. (12.8–12.9)).

Appendix sections

12.5.1 Slutsky equation, substitution effect, and income effect

The influence of a change in price on the demand for goods can be decomposed into an income effect and a substitution effect as mentioned in the main text. This is known as Hicksian decomposition or the Slutsky equation [8].

When given a utility function $u(\mathbf{x})$, we define $\hat{x}_i(\mathbf{p}, I)$ as the optimal demand for good i determined as a function of the price of the good $\mathbf{p}$ and income I. By defining $E(\mathbf{p}, u)$ as "the minimum income required to achieve a certain utility value u," we can represent "the minimum demand for good i required to achieve a utility value u" as $h_i(\mathbf{p}, u) := \hat{x}_i(\mathbf{p}, E(\mathbf{p}, u))$.

Differentiating this function $h_i(\mathbf{p}, u)$ with respect to p_j yields

$$\frac{\partial h_i(\mathbf{p}, \hat{u}(\mathbf{p}, I))}{\partial p_j} = \frac{\partial \hat{x}_i(\mathbf{p}, I)}{\partial p_j} + \frac{\partial \hat{x}_i(\mathbf{p}, I)}{\partial I} \frac{\partial E(\mathbf{p}, \hat{u}(\mathbf{p}, I))}{\partial p_j},$$

where $\hat{u}(\mathbf{p}, I)$ represents the maximum utility under a given price $\mathbf{p}$ and income I. Due to optimality, the last term $\partial E(\mathbf{p}, \hat{u}(\mathbf{p}, I))/\partial p_j$ equals to the optimal demand $\hat{x}_j(\mathbf{p}, I)$.

Accordingly, we obtain the Slutsky equation that describes the response of demand $\hat{x}_i(\mathbf{p}, I)$ to changes in price p_j:

$$\frac{\partial \hat{x}_i(\mathbf{p}, I)}{\partial p_j} = \frac{\partial h_i(\mathbf{p}, \hat{u}(\mathbf{p}, I))}{\partial p_j} - \hat{x}_j(\mathbf{p}, I) \frac{\partial \hat{x}_i(\mathbf{p}, I)}{\partial I}. \tag{12.19}$$

The first term $\partial h_i(\mathbf{p}, \hat{u})/\partial p_j$ represents the substitution effect caused by relative changes in the price of each good; particularly, the "self-substitution effect" for $i = j$ is always non-positive [8]. In contrast, the second term $\hat{x}_j(\mathbf{p}, I) \frac{\partial \hat{x}_i(\mathbf{p}, I)}{\partial I}$ reflects the income effect, which can be either positive or negative. This represents the effect that an increase in the price of a good leads to an effective decrease in income, which also changes the demand for goods. Eq. (12.19) states that these two effects determine the dependence of the demand for goods on the price (see also Box 12.A).

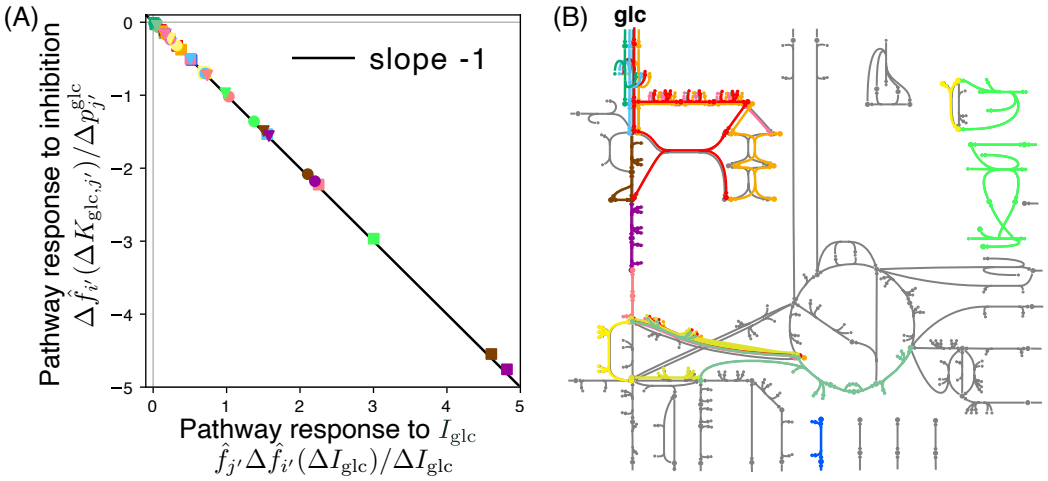

Figure 12.8: Responses of the optimized pathway fluxes $\hat{\mathbf{f}}$. (A) Responses to metabolic inhibitions, $\Delta\hat{f}_{i'}(\Delta K_{\mathrm{glc},j'})/\Delta p^{\mathrm{glc}}_{j'}$, are plotted against the nutrient responses, $\hat{f}_{j'}\Delta\hat{f}_{i'}(\Delta I_{\mathrm{glc}})/\Delta I_{\mathrm{glc}}$. All different shapes and colors of markers represent different i' and j', respectively. $I_{\mathrm{glc}} = 5\,[\mathrm{mmol/gDW/h}]$. (B) 13 active extreme pathways, computed using efmtool [57], are shown. Colors correspond to those of the markers for manipulated pathways j' in panel A. The whole metabolic network of the *E. coli* core model is shown in gray. Here, (linear sums of) EFMs or extreme pathways for the stoichiometry without objective reaction o are considered as the metabolic pathways. That is, we consider metabolic pathways from components α with influxes $I_\alpha > 0$ to objective components $\mathcal{O}$. (Modified from Ref. [5]).

12.5.2 Derivation of Eq. (12.15) using the implicit function theorem

Let us assume a non-degenerate optimum, i.e., the optimal solution $\hat{\mathbf{f}}(K, \mathbf{I})$ is locally unique in a neighborhood of the given parameter, $(K, \mathbf{I})$. Then, the set $\mathcal{B}\,(\subset \mathcal{E}\cup\mathcal{C})$ of active inequality constraints (called binding constraints) remains unchanged, and the matrix corresponding to these binding constraints, denoted by $K_{\mathcal{B}}$, is of full rank. In this case, the binding constraints can be written as equalities,

$$g_\alpha\big(\hat{\mathbf{f}}(K,\mathbf{I}), K, \mathbf{I}\big) := \sum_{j'\in\mathcal{P}} K_{\alpha j'}\,\hat{f}_{j'}(K,\mathbf{I}) + I_\alpha = 0 \quad (\alpha\in\mathcal{B}). \tag{12.20}$$

Collecting g_α into a vector $\mathbf{g} := \{g_\alpha\}_{\alpha\in\mathcal{B}}$, the above Eq. (12.20) can be written compactly as

$$\mathbf{g}\big(\hat{\mathbf{f}}(K,\mathbf{I}), K, \mathbf{I}\big) = \mathbf{0}. \tag{12.21}$$

Differentiating Eq. (12.21) with respect to the nutrient availability I_ν and applying the implicit function theorem, we obtain

$$\frac{\partial\mathbf{g}}{\partial\hat{\mathbf{f}}}\,\frac{\partial\hat{\mathbf{f}}}{\partial I_\nu} + \frac{\partial\mathbf{g}}{\partial I_\nu} = \mathbf{0}. \tag{12.22}$$

Since $\partial\mathbf{g}/\partial\hat{\mathbf{f}} = K_{\mathcal{B}}$, Eq. (12.22) yields

$$\frac{\partial\hat{\mathbf{f}}}{\partial I_\nu} = -K_{\mathcal{B}}^{-1}\,\mathbf{e}_\nu, \tag{12.23}$$

where $\mathbf{e}_\nu := \partial\mathbf{g}/\partial I_\nu$ is the unit vector in the direction of ν (if $\nu\in\mathcal{B}$, and zero otherwise).

Similarly, differentiating Eq. (12.21) with respect to the stoichiometric coefficient $K_{\nu j'}$ gives

$$\frac{\partial\mathbf{g}}{\partial\hat{\mathbf{f}}}\,\frac{\partial\hat{\mathbf{f}}}{\partial K_{\nu j'}} + \frac{\partial\mathbf{g}}{\partial K_{\nu j'}} = \mathbf{0}.$$

Using $\partial \mathbf{g}/\partial \hat{\mathbf{f}} = K_{\mathcal{B}}$ and $\partial \mathbf{g}/\partial K_{\nu j'} = \hat{f}_{j'}(K, \mathbf{I})\, \mathbf{e}_\nu$, we obtain

$$\frac{\partial \hat{\mathbf{f}}}{\partial K_{\nu j'}} = -K_{\mathcal{B}}^{-1}\, \hat{f}_{j'}(K, \mathbf{I})\, \mathbf{e}_\nu. \tag{12.24}$$

Eliminating $K_{\mathcal{B}}^{-1}\mathbf{e}_\nu$ between Eqs. (12.23-12.24) yields

$$\frac{\partial \hat{f}_{i'}(K, \mathbf{I})}{\partial K_{\nu j'}} = \hat{f}_{j'}(K, \mathbf{I})\, \frac{\partial \hat{f}_{i'}(K, \mathbf{I})}{\partial I_\nu}, \tag{12.25}$$

which is exactly Eq. (12.15), noting that the metabolic price is defined as $p^\nu_{j'} = -K_{\nu j'}$.

12.5.3 Derivation of Eq. (12.16) from Eq. (12.15)

Noting $\hat{\mathbf{v}} = P\hat{\mathbf{f}}$ and multiplying Eq. (12.15) by pathway matrix P from the left, we immediately obtain equality for the responses of reaction fluxes $\mathbf{v}$:

$$\frac{\partial \hat{v}_i(K, \mathbf{I})}{\partial p^\nu_{j'}} = -f_{j'}(K, \mathbf{I}) \frac{\partial \hat{v}_i(K, \mathbf{I})}{\partial I_\nu} \quad (i \in \mathcal{R},\ j' \in \mathcal{P}), \tag{12.26}$$

Assuming that a stoichiometric coefficient $S_{\mu j}$ of reaction j is effectively altered to $S_{\mu j} - \Delta S_{\mu j}$, the j'-th column vector of matrix $K := SP$ changes as

$$\begin{aligned} \{K_{\alpha j'}\}_{\alpha \in \mathcal{M}\cup\mathcal{C}} \quad &\to \quad \{K_{\alpha j'} - \Delta K_{\alpha j'}\}_{\alpha \in \mathcal{M}\cup\mathcal{C}} \\ &:= \{\sum_{k\in\mathcal{R}} S_{\alpha k} P_{k j'} - \delta_{\alpha\mu} \Delta S_{\mu j} P_{j j'}\}_{\alpha \in \mathcal{M}\cup\mathcal{C}}, \end{aligned}$$

with Kronecker delta $\delta_{\alpha\mu}$. That is, the metabolic price of pathway j' for metabolite μ changes by $\Delta p^\mu_{j'} = \Delta S_{\mu j} P_{j j'}$.

Therefore, if multiple stoichiometric coefficients are simultaneously altered,

$$\begin{aligned} \Delta \hat{v}_i(\{\Delta S_{\alpha j}\}_{\alpha\in\mathcal{M}\cup\mathcal{C}}) \quad &= \quad \sum_{\mu\in\mathcal{M}} \sum_{j'\in\mathcal{P}} \frac{\partial \hat{v}_i(K, \mathbf{I})}{\partial p^\mu_{j'}} \Delta p^\mu_{j'} \\ &= \quad \sum_{\mu\in\mathcal{M}} \sum_{j'\in\mathcal{P}} \frac{\partial \hat{v}_i(K, \mathbf{I})}{\partial p^\mu_{j'}} P_{j j'} \Delta S_{\mu j}. \end{aligned}$$

From Eq. (12.26) and $\hat{\mathbf{v}} = P\hat{\mathbf{f}}$,

$$\begin{aligned} \Delta \hat{v}_i(\{\Delta S_{\alpha j}\}_{\alpha\in\mathcal{M}\cup\mathcal{C}}) \quad &= \quad -\sum_{\mu\in\mathcal{M}} \sum_{j'\in\mathcal{P}} \Delta S_{\mu j} P_{j j'} \hat{f}_{j'} \frac{\partial \hat{v}_i}{\partial I_\mu}. \\ &= \quad -\hat{v}_j \sum_{\mu\in\mathcal{M}} \Delta S_{\mu j} \frac{\partial \hat{v}_i}{\partial I_\mu}. \end{aligned} \tag{12.27}$$

Then, by defining $c^\nu_\mu(i) := \frac{\partial \hat{v}_i}{\partial I_\mu} / \frac{\partial \hat{v}_i}{\partial I_\nu}$ and

$$\Delta q^\nu_i(\{\Delta S_{\mu i}\}_{\mu\in\mathcal{M}}) := \sum_{\mu\in\mathcal{M}} c^\nu_\mu(i) \Delta S_{\mu i}$$

and applying it to Eq. (12.27) in the case of $j = i$, we obtain

$$\Delta \hat{v}_i(\{\Delta S_{\alpha j}\}_{\alpha\in\mathcal{M}\cup\mathcal{C}}) = -\hat{v}_i \frac{\partial \hat{v}_i}{\partial I_\nu} \underbrace{\sum_{\mu\in\mathcal{M}} c^\nu_\mu(i) \Delta S_{\mu i}}_{=:\Delta q^\nu_i}.$$

Finally, Eq. (12.16) is derived:

$$\frac{\partial \hat{v}_i(S, \mathbf{I})}{\partial q^\nu_i} = -\hat{v}_i(S, \mathbf{I}) \frac{\partial \hat{v}_i(S, \mathbf{I})}{\partial I_\nu}.$$

Although the precise calculation of the coefficients $c_\mu^\nu(i)$ requires information regarding not only the responses of $\hat{v}_i$ to I_ν but also those to I_μ, they can be approximated in ways easier and independent of reaction i. For example, under extreme situations in which only the carbon sources limit the objective reaction, c_μ^ν should be the ratios of the carbon numbers of compounds μ and ν; alternatively, the simplest approximation could be just taking c_μ^ν as unities. Even with these approximations, the relation (12.16) appears to hold well, and thus such approximations will be useful for qualitatively predicting whether metabolic inhibition promotes or suppresses the reaction of interest (see Supplementary Material of Ref. [5] for details).

Solutions to problems

Problem 12.1 (Analysis of the coarse-grained model in Section 12.2)

Hint: The ridgeline of the growth rate landscape (shown in dashed gray line in Figure 12.1B) is given by $f_\mathrm{f} = -\frac{1+b_\mathrm{r}}{1+b_\mathrm{f}}\frac{a_\mathrm{r}}{a_\mathrm{f}}f_\mathrm{r} + \frac{J_{B,\mathrm{tot}}}{a_\mathrm{f}(1+b_\mathrm{f})}$.

Problem 12.2 (Proof of convexity in CBM)

Hint: Use the duality and strong duality theorem.

Bibliography

[1] Paul A Samuelson. *Economics: an Introductory Analysis*. McGraw-Hill, 1948. URL https://books.google.co.jp/books?id=ITXUAAAAMAAJ.

[2] Dan Ariely. *Predictably irrational*. HarperCollins, United States, 2008. ISBN 978-0-06-135323-9.

[3] Rafael U Ibarra, Jeremy S Edwards, and Bernhard O Palsson. Escherichia coli k-12 undergoes adaptive evolution to achieve in silico predicted optimal growth. *Nature*, 420(6912):186–189, 2002.

[4] Jumpei F. Yamagishi and Tetsuhiro S. Hatakeyama. Microeconomics of Metabolism: The Warburg Effect as Giffen Behaviour. *Bulletin of Mathematical Biology*, 83(12):120, October 2021. ISSN 1522-9602. doi: 10.1007/s11538-021-00952-x.

[5] Jumpei F Yamagishi and Tetsuhiro S Hatakeyama. Linear response theory of evolved metabolic systems. *Physical Review Letters*, 131(2):028401, 2023.

[6] Jumpei F Yamagishi and Tetsuhiro S Hatakeyama. Global constraint model for microbial growth laws. *Proceedings of the National Academy of Sciences*, 122(40):e2515031122, 2025.

[7] Wim Heijman and Pierre von Mouche, editors. *New Insights into the Theory of Giffen Goods*, volume 655 of *Lecture Notes in Economics and Mathematical Systems*. Springer Berlin Heidelberg, Heidelberg, 2012. ISBN 978-3-642-21776-0 (print); 978-3-642-21777-7 (electronic).

[8] Hal R Varian. *Microeconomic analysis*. WW Norton, New York, 1992.

[9] Kelvin J Lancaster. A new approach to consumer theory. *Journal of political economy*, 74(2):132–157, 1966.

[10] Anjan Roy, Dotan Goberman, and Rami Pugatch. A unifying autocatalytic network-based framework for bacterial growth laws. *Proceedings of the National Academy of Sciences*, 118(33):e2107829118, 2021.

[11] Chen Liao, Tong Wang, Sergei Maslov, and Joao B Xavier. Modeling microbial cross-feeding at intermediate scale portrays community dynamics and species coexistence. *PLoS Computational Biology*, 16(8):e1008135, 2020.

[12] M. Basan, S. Hui, H. Okano, Z. Zhang, Y Shen, J.R. Williamson, and T. Hwa. Overflow metabolism in Escherichia coli results from efficient proteome allocation. *Nature*, 528:99, 2015. doi: 10.1038/nature15765.

[13] Matteo Mori, Terence Hwa, Olivier C. Martin, Andrea De Martino, and Enzo Marinari. Constrained allocation flux balance analysis. *PLoS computational biology*, 12(6):e1004913, 2016. doi: 10.1371/journal.pcbi.1004913.

[14] Alexei Vazquez, Jiangxia Liu, Yi Zhou, and Zoltán N Oltvai. Catabolic efficiency of aerobic glycolysis: the warburg effect revisited. *BMC Systems Biology*, 4(1):1–9, 2010.

[15] Alexei Vazquez. *Overflow metabolism: from yeast to marathon runners*. Academic Press, London, 2017.

[16] M. Szenk, K. A. Dill, and A. M. R. de Graff. Why do fast-growing bacteria enter overflow metabolism? testing the membrane real estate hypothesis. *Cell Systems*, 5(2):95–104, 2017.

[17] Bastian Niebel, Simeon Leupold, and Matthias Heinemann. An upper limit on gibbs energy dissipation governs cellular metabolism. *Nature Metabolism*, 1(1):125, January 2019. doi: 10.1038/s42255-018-0006-7.

[18] Yihui Shen, Hoang V Dinh, Edward R Cruz, Zihong Chen, Caroline R Bartman, Tianxia Xiao, Catherine M Call, Rolf-Peter Ryseck, Jimmy Pratas, Daniel Weilandt, et al. Mitochondrial atp generation is more proteome efficient than glycolysis. *Nature chemical biology*, 20(9):1123–1132, 2024.

[19] Daan H De Groot, Julia Lischke, Riccardo Muolo, Robert Planqué, Frank J Bruggeman, and Bas Teusink. The common message of constraint-based optimization approaches: overflow metabolism is caused by two growth-limiting constraints. *Cellular and Molecular Life Sciences*, 77:441–453, 2020. doi: 10.1007/s00018-019-03380-2.

[20] Cornelis Verduyn, Erik Postma, W Alexander Scheffers, and Johannes P Van Dijken. Effect of benzoic acid on metabolic fluxes in yeasts: a continuous-culture study on the regulation of respiration and alcoholic fermentation. *Yeast*, 8(7):501–517, 1992.

[21] Bernhard Ø. Palsson. *Systems Biology: Constraint-Based Reconstruction and Analysis*. Cambridge University Press, 2015.

[22] E. Klipp, W. Liebermeister, C. Wierling, and A. Kowald. *Systems Biology: a textbook*. John Wiley & Sons, New Jersey, 2016.

[23] Tom J Clement, Erik B Baalhuis, Bas Teusink, Frank J Bruggeman, Robert Planqué, and Daan H de Groot. Unlocking elementary conversion modes: Ecmtool unveils all capabilities of metabolic networks. *Patterns*, 2(1), 2021.

[24] Jeffrey D Orth, Ronan MT Fleming, and Bernhard Ø Palsson. Reconstruction and use of microbial metabolic networks: the core escherichia coli metabolic model as an educational guide. *EcoSal plus*, 4(1):10–1128, 2010.

[25] George Stephanopoulos, Aristos A Aristidou, and Jens Nielsen. *Metabolic engineering: principles and methodologies*. Elsevier, Amsterdam, 1998.

[26] Robert Schuetz, Lars Kuepfer, and Uwe Sauer. Systematic evaluation of objective functions for predicting intracellular fluxes in Escherichia coli. *Molecular systems biology*, 3(1):119, 2007.

[27] Erwin P Gianchandani, Matthew A Oberhardt, Anthony P Burgard, Costas D Maranas, and Jason A Papin. Predicting biological system objectives de novo from internal state measurements. *BMC Bioinformatics*, 9(1):1–13, 2008.

[28] Yu Chen and Jens Nielsen. Yeast has evolved to minimize protein resource cost for synthesizing amino acids. *Proceedings of the National Academy of Sciences*, 119(4):e2114622119, 2022.

[29] Manabu Kodama, Kiyotaka Oshikawa, Hideyuki Shimizu, Susumu Yoshioka, Masatomo Takahashi, Yoshihiro Izumi, Takeshi Bamba, Chisa Tateishi, Takeshi Tomonaga, Masaki Matsumoto, et al. A shift in glutamine nitrogen metabolism contributes to the malignant progression of cancer. *Nature communications*, 11(1):1320, 2020.

[30] Ralph J DeBerardinis, Anthony Mancuso, Evgueni Daikhin, Ilana Nissim, Marc Yudkoff, Suzanne Wehrli, and Craig B Thompson. Beyond aerobic glycolysis: transformed cells can engage in glutamine metabolism that exceeds the requirement for protein and nucleotide synthesis. *Proceedings of the National Academy of Sciences*, 104 (49):19345–19350, 2007.

[31] Johannes a Meiser, Sergey Tumanov, Oliver Maddocks, Christian F Labuschagne, Eyal Gottlieb, Karen Blyth, Karen Vousden, et al. Serine one-carbon catabolism with formate overflow. *Science advances*, 2(10):e1601273, 2016.

[32] Cédric Chaveroux, Carmen Sarcinelli, Virginie Barbet, Sofiane Belfeki, Audrey Barthelaix, Carole Ferraro-Peyret, Serge Lebecque, Toufic Renno, Alain Bruhat, Pierre Fafournoux, et al. Nutrient shortage triggers the hexosamine biosynthetic pathway via the gcn2-atf4 signalling pathway. *Scientific reports*, 6(1):27278, 2016.

[33] Avi Flamholz, Elad Noor, Arren Bar-Even, Wolfram Liebermeister, and Ron Milo. Glycolytic strategy as a tradeoff between energy yield and protein cost. *Proc. Natl. Acad. Sci. U. S. A.*, 110(24):10039–10044, June 2013. doi: 10.1073/pnas.1215283110.

[34] Toru Jojima, Takafumi Igari, Ryoji Noburyu, Akira Watanabe, Masako Suda, and Masayuki Inui. Coexistence of the entner–doudoroff and embden–meyerhof pathways in corynebacterium glutamicum leads to efficient assimilation of glucose in corynobacterial cell factories. *Biotechnology for Biofuels*, 14:1–9, 2021.

[35] Terence D Thomas, Derek C Ellwood, and V Michael C Longyear. Change from homo-to heterolactic fermentation by streptococcus lactis resulting from glucose limitation in anaerobic chemostat cultures. *Journal of bacteriology*, 138(1):109–117, 1979.

[36] Hugh AL Henry and Lonnie W Aarssen. On the relationship between shade tolerance and shade avoidance strategies in woodland plants. *Oikos*, pages 575–582, 1997.

[37] Jacques Monod. The growth of bacterial cultures. *Annual Reviews in Microbiology*, 3(1):371–394, 1949.

[38] J.G. Reich and E.E. Selkov. *Energy metabolism of the cell : a theoretical treatise*. Academic Press, London ; New York, 1981. ISBN 0125859201.

[39] D. Sher, D. Segrè, and M. J. Follows. Quantitative principles of microbial metabolism shared across scales. *Nature Microbiology*, pages 1–14, 2024.

[40] Y. Liu. Overview of some theoretical approaches and modeling for microbial growth. *Applied Microbiology and Biotechnology*, 73(6):1241–1250, 2007.

[41] Hidde De Jong, Stefano Casagranda, Nicola Giordano, Eugenio Cinquemani, Delphine Ropers, Johannes Geiselmann, and Jean-Luc Gouzé. Mathematical modelling of microbes: metabolism, gene expression and growth. *Journal of The Royal Society Interface*, 14(136):20170502, 2017.

[42] J. C. Merchuk and J. A. Asenjo. Monod equation and microbial growth. *Biotechnology Progress*, 11(1):93–98, 1995.

[43] Q. Jin and C. M. Bethke. A new form of the monod equation for describing the growth of bacteria in batch and continuous cultures. *Geochimica et Cosmochimica Acta*, 67(17):3189–3203, 2003.

[44] J. J. Heijnen and B. Romein. Derivation of kinetic expressions for growth on mixtures of substrates. *Biotechnology and Bioengineering*, 48(6):616–628, 1995.

[45] Arthur L. Koch. *Microbial physiology and ecology of slow-growing bacteria*. Springer, 1997.

[46] Anne Goelzer, Vincent Fromion, and Gérard Scorletti. Cell design in bacteria as a convex optimization problem. *Automatica*, 47(6):1210–1218, 2011. doi: 10.1016/j.automatica.2011.02.038.

[47] A. Bren, J. O. Park, B. D. Towbin, E. Dekel, J. D. Rabinowitz, and U. Alon. Glucose becomes one of the worst carbon sources for e. coli on poor nitrogen sources due to suboptimal levels of camp. *Scientific Reports*, 6(1):24834, 2016.

[48] Jinyun Tang and William J. Riley. Finding Liebig's law of the minimum. *Ecological Applications*, 31(8):e02458, 2021. ISSN 1051-0761. doi: 10.1002/eap.2458. Publisher: John Wiley & Sons, Ltd.

[49] U. Sommer. Comparison and modeling of microbial growth kinetics on various substrates. *Microbial Ecology*, 22 (1):1–10, 1991.

[50] K. Kovárová-Kovar and T. Egli. Growth kinetics of suspended microbial cells: from single-substrate-controlled growth to mixed-substrate kinetics. *Microbiology and Molecular Biology Reviews*, 62(3):646–666, 1998.

[51] H. Wang, P. V. Garcia, S. Ahmed, and C. M. Heggerud. Mathematical comparison and empirical review of the monod and droop forms for resource-based population dynamics. *Ecological Modelling*, 466:109887, 2022.

[52] Christer Larsson, Urs von Stockar, Ian Marison, and Lena Gustafsson. Growth and metabolism of saccharomyces cerevisiae in different carbon-, nitrogen-, or carbon-and nitrogen-limiting conditions. *Journal of bacteriology*, 175 (15):4809–4816, 1993.

[53] J. D. Orth, T. M. Conrad, J. Na, J. A. Lerman, H. Nam, A. M. Feist, and Bernhard Ø. Palsson. A comprehensive genome-scale reconstruction of escherichia coli metabolism—2011. *Molecular Systems Biology*, 7(1):535, 2011.

[54] A. Ebrahim, J. A. Lerman, Bernhard Ø. Palsson, and D. R. Hyduke. Cobrapy: Constraints-based reconstruction and analysis for python. *BMC Syst Biol*, 7, 2013.

[55] Jumpei F Yamagishi and Tetsuhiro S Hatakeyama. Thermodynamic cost-controllability tradeoff in metabolic currency coupling. *arXiv:2602.01604*, 2026.

[56] Paul A Samuelson. *Foundations of Economic Analysis*. Harvard University Press, Cambridge, MA, enlarged edition edition, 1983. ISBN 9780674313033. Originally published 1947.

[57] Marco Terzer and Jörg Stelling. Large-scale computation of elementary flux modes with bit pattern trees. *Bioinformatics*, 24(19):2229–2235, 2008. ISSN 1367-4803. doi: 10.1093/bioinformatics/btn401.